processes

MDPI

Article

Identification of Control Parameters for Converters of Doubly Fed Wind Turbines Based on Hybrid Genetic Algorithm

Linlin Wu [1], Hui Liu [1], Jiaan Zhang [2,*], Chenyu Liu [3,*], Yamin Sun [1], Zhijun Li [2] and Jingwei Li [3]

[1] State Grid Jibei Electric Power Co., Ltd., Research Institute, Beijing 100045, China; wulin226@163.com (L.W.); liuhtj@163.com (H.L.); sunyamin8888@163.com (Y.S.)
[2] State Key Laboratory of Reliability and Intelligence of Electrical Equipment, Hebei University of Technology, Tianjin 300130, China; zhijun_li@263.net
[3] College of Artificial Intelligence and Data Science, Hebei University of Technology, Tianjin 300401, China; tpcnljwyx@163.com
* Correspondence: 2011086@hebut.edu.cn (J.Z.); liuchenyux@163.com (C.L.)

Abstract: The accuracy of doubly fed induction generator (DFIG) models and parameters plays an important role in power system operation. This paper proposes a parameter identification method based on the hybrid genetic algorithm for the control system of DFIG converters. In the improved genetic algorithm, the generation gap value and immune strategy are adopted, and a strategy of "individual identification, elite retention, and overall identification" is proposed. The DFIG operation data information used for parameter identification considers the loss of rotor current, stator current, grid-side voltage, stator voltage, and rotor voltage. The operating data of a wind farm in Zhangjiakou, North China, were used as a test case to verify the effectiveness of the proposed parameter identification method for the Maximum Power Point Tracking (MPPT), constant speed, and constant power operation conditions of the wind turbine.

Keywords: wind power; doubly fed induction generator; parameter identification; immune algorithm; genetic algorithm

Citation: Wu, L.; Liu, H.; Zhang, J.; Liu, C.; Sun, Y.; Li, Z.; Li, J. Identification of Control Parameters for Converters of Doubly Fed Wind Turbines Based on Hybrid Genetic Algorithm. *Processes* **2022**, *10*, 567. https://doi.org/10.3390/pr10030567

Academic Editors: Jie Zhang and Meihong Wang

Received: 27 January 2022
Accepted: 12 March 2022
Published: 14 March 2022

1. Introduction

Considering the depletion of fossil fuels and the threat that greenhouse gas emissions pose to the global climate, the proportion of renewable energy will continue to expand [1], and wind power is poised to be a major contributor to this expansion. Owing to the different structures, types, and capacities of wind turbines, the control system strategy and parameters will also be different, resulting in different power generation characteristics [2]. As large-scale wind turbine integration will greatly affect the stability of the power system, the accuracy of the power system model has become an important technical issue in the operation, which needs to be consistent with the physical system, and the accuracy of the parameters is the key to ensuring model correctness. Parameter identification is a feasible method for model acquisition during the test and operation of wind turbines.

At present, the doubly fed induction generator (DFIG) is one of the main wind turbine types used on the market. The research on parameter identification of the DFIG has mainly focused on electrical parameters [3] and parameters of the converter control system. Classified from the perspective of algorithms, it can be divided into two types: traditional statistical algorithms and intelligent algorithms. In [4], an Extended Kalman Filter (EKF) was proposed for parameter estimation of DFIG in wind turbine systems. Belmokhtar et al. [5] explored the recursive least-squares (RLS) online parameter identification of a DFIG operating in a wind energy conversion system. Based on the RLS, a two-stage identification method was applied in [6], and the correctness of the method was verified by simulation. Wang et al. [7] applied the damped least-squares algorithm to identify the parameters of a variable speed DFIG-based wind turbine generator for wind

power dynamic analysis. Takahashi et al. [8] proposed a recursive least-squares sensorless identification method for online identification of permanent magnet synchronous generator parameters, and it effectively detects characteristic changes during aging and degradation. A new decoupled weighted recursive least-squares (DWRLS) method, proposed in [9], improves the modeling accuracy by separately estimating the parameters of the fast and slow dynamics. Xia et al. [10] improved the model's parameter discrimination accuracy based on forgetting the factor recursive least squares for the state-of-charge (SOC) estimation of a battery management system.

Most traditional identification methods require that the input signal is known and varies significantly. For some situations or systems, it may not be possible to obtain all necessary input signals accurately, making the method less adaptable. Especially for nonlinear systems, this often leads to low identification accuracy or poor global search ability. Therefore, some bionic optimization algorithms, which have been developed and applied to research on parameter identification, have gradually formed the current intelligent parameter identification method [11]. These methods include the artificial neural network, particle swarm optimization algorithm, and genetic algorithm.

Based on the artificial neural network method, Rong et al. [12] proposed a step-by-step identification strategy to get the electrical parameters of a generator. In [13], a performance evaluation model was constructed with long short-term memory (LSTM) neural units and auto-encoder (AE) networks to evaluate the degree of abnormal performance of wind turbines, and an adaptive threshold estimation method was established to identify key condition-monitoring parameters. Based on the particle swarm algorithm, Li et al. [14] realized the dynamic equivalence of multiple units and simplified the equivalent values of the electrical parameters for multi-wind turbines. In [15], a new method for estimating the parameters of a wind turbine DFIG and drivetrain system was proposed, and the global optimal estimation result was obtained based on the local estimation and the coordinated estimation method under different types of disturbances. In [16], a symbolic regression method was introduced to identify models of a horizontal-axis wind turbine with evolutionary multi-objective optimization. In [17], wind turbine structural parameters such as inertial parameters, the damping coefficient, axial strength, and gearbox damping ratio were identified based on the genetic algorithm. In [18], different control modes of wind turbines under different lower voltage levels were identified based on the genetic algorithm. In [19], the objective function was to minimize the active output power error between the equivalent model and the actual wind farm, and an improved genetic algorithm was used to identify the key parameters of a permanent magnet synchronous generator. In [20], a set of fan parameters was identified with fault record data and the genetic algorithm to identify, and the evaluation function was to calculate the total deviation between the original signal and the simulation result.

The local search ability of the traditional genetic algorithm is insufficient and prone to premature convergence. Consequently, the relevant parameters of an excitation system were decomposed into multiple sets in [21], and a niche genetic algorithm with a fitness-sharing mechanism was proposed to overcome the local convergence for parameters identification. In view of the particularity of the DFIG structure and the complexity of its inverter control system, in this paper, the generation gap value and immune strategy are applied, and a strategy to improve the parameter identification based on the genetic algorithm is introduced, namely "individual identification, elite retention and overall identification", so as to establish a hybrid genetic algorithm (HGA) suitable for parameter identification of the DFIG converter control system. It is also considered that data variables used for DFIG parameter identification, such as rotor current, stator current, grid voltage, stator voltage, and rotor voltage, may be missing during the operation of the wind farm.

2. DFIG Converter Control Model and Parameters to Be Identified

2.1. Converter Control Model and its Parameters to Be Identified

DFIG has been widely used in wind power systems and is mainly composed of a wind turbine, transmission chain system, wound induction generator, and control system [22]. Figure 1 shows the structure of the DFIG-based wind power generation system, where the stator windings are directly connected to the grid and the rotor windings are directly connected to the external power grid through back-to-back converters [23]. The back-to-back converter provides three-phase rotor excitation power with adjustable amplitude, frequency, and phase, and ensures that the slip power can flow in both directions.

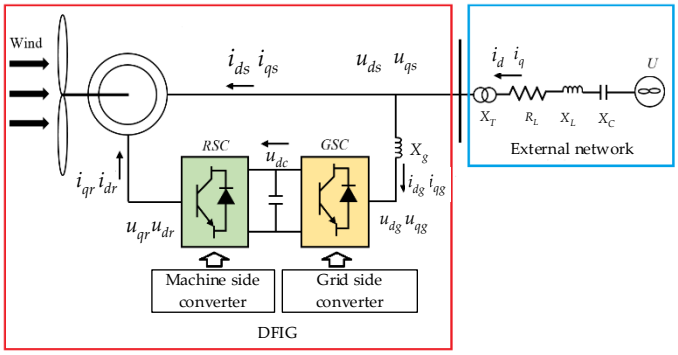

Figure 1. Structure of doubly fed induction generator (DFIG)-based wind power generation system.

The converter of the doubly fed wind turbine consists of a rotor-side converter (RSC) and a grid-side converter [23]. The RSC realizes the variable speed and constant frequency operation of the DFIG by controlling the rotor excitation current, while the grid side converter (GSC) maintains the DC bus voltage constant by controlling the power output. Because the control objectives of the RSC and the GSC are different, the RSC adopts the stator flux linkage-oriented control method, while the GSC adopts the vector control method based on the grid voltage orientation. Figure 2a shows a block diagram of a typical control system of the RSC of a doubly fed wind turbine, which is a double closed-loop structure composed of an outer power loop and an inner current loop to realize active and reactive power decoupling control. Figure 2b shows the typical control system block diagram of the GSC of the DFIG, which is a double closed-loop structure of the DC voltage outer loop and the grid-connected current inner loop. The DC voltage outer loop is used to realize the DC voltage. The stable control of the innercurrent loop is used to achieve fast tracking of active current and reactive current.

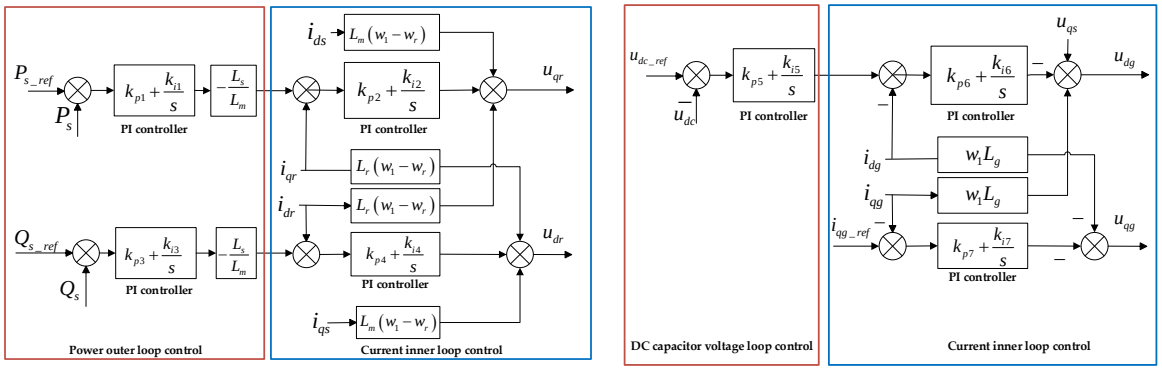

Figure 2. Control strategy diagram of the converter. (**a**) Typical control system block diagram of the rotor-side converter (RSC); (**b**) Typical control system block diagram of the grid side converter (GSC).

It can be known from the current inner loop control flow in Figure 2a that the output expression of the double closed-loop PI controller of the rotor-side converter is as follows:

$$\begin{cases} u_{dr} = \frac{dx_4}{dt}(k_{p4} + \frac{k_{i4}}{s}) - L_r(\omega_1 - \omega_r)i_{qr} - L_m(\omega_1 - \omega_r)i_{qs} \\ u_{qr} = \frac{dx_2}{dt}(k_{p2} + \frac{k_{i2}}{s}) + L_r(\omega_1 - \omega_r)i_{dr} + L_m(\omega_1 - \omega_r)i_{ds} \end{cases}, \quad (1)$$

where k_{p2} and k_{p4} are the proportional coefficients, while k_{i2} and k_{i4} are the integral coefficients, which are in the two PI controllers of RSC. L_r and L_m are the inductance of the rotor winding and the mutual inductance between the stator winding and the rotor winding, respectively. w_1 and w_r are the synchronous speed and the rotor speed of the wind turbine, respectively. i_{dr} and i_{qr} are respectively the d-axis and q-axis components of the rotor current in the dp coordinate system. x_4 and x_2 are state variables.

As the current inner loop control flow in Figure 2b shows, the output expression of the double closed-loop PI controller of the grid-side converter is as follows:

$$\begin{cases} u_{dg} = u_{qs} - \frac{dx_6}{dt}(k_{p6} + \frac{k_{i6}}{s}) + \omega_1 L_g i_{qg} \\ u_{qg} = -\frac{dx_7}{dt}(k_{p7} + \frac{k_{i7}}{s}) - \omega_1 L_g i_{dg} \end{cases}, \quad (2)$$

where k_{p6}, k_{p7} and k_{i6}, k_{i7} are the proportional and integral parameters of the two PI controllers of the grid-side converter, respectively. L_g is the filter inductor on the grid side. i_{dg} and i_{qg} are the d-axis and q-axis components of the grid-side current in the dp coordinate system, respectively. x_6 and x_7 are state variables.

In Equations (1) and (2), the expressions of the state variables, x_2, x_4, x_6, and x_7 are shown in Equations (3) and (4), representing the rotor side and grid side, respectively.

$$\begin{cases} \frac{dx_1}{dt} = P_{s\_ref} - P_s \\ \frac{dx_2}{dt} = \frac{dx_1}{dt}(k_{p1} + \frac{k_{i1}}{s})(-\frac{L_s}{L_m}) - i_{qr} \\ \frac{dx_3}{dt} = Q_{s\_ref} - Q_s \\ \frac{dx_4}{dt} = \frac{dx_3}{\mathrm{dt}}(k_{p3} + \frac{k_{i3}}{s})(-\frac{L_s}{L_m}) + \frac{U_s}{\omega_1 L_m} - i_{dr} \end{cases}, \quad (3)$$

$$\begin{cases} \frac{dx_5}{dt} = u_{dc\_ref} - u_{dc} \\ \frac{dx_6}{dt} = \frac{dx_5}{dt}(k_{p5} + \frac{k_{i5}}{s}) - i_{dg} \\ \frac{dx_7}{dt} = i_{qg\_\mathrm{ref}} - i_{qg} \end{cases}. \quad (4)$$

In Equation (3), k_{p1} and k_{i1} are the proportional and integral parameters of the active power outer loop PI controller, respectively. k_{p3} and k_{i3} are the proportional and integral parameters of the reactive power outer loop PI controller, respectively. P_{s_ref}, P_s, Q_{s_ref}, and Q_s are the systemic active power reference value, active power output value, reactive power reference value, and reactive power output value, respectively. U_s represents the stator winding voltage, $u_{ds}^2 + u_{qs}^2 = U_s^2$. x_1, x_2, x_3, and x_4 are intermediate state variables.

In Equation (4), k_{p5} and k_{i5} are the proportional and integral parameters of the DC bus voltage outer loop PI control, respectively. u_{dc_ref} and u_{dc} are the DC bus voltage reference value and the DC bus voltage output value, respectively. i_{dg}, iq_{g_ref}, and i_{qg} are the d-axis components of the grid-side current, and the reference value of the q-axis components and the q-axis components are in the dp coordinate system. x_5, x_6, and x_7 are intermediate state variables.

In the converter parameter identification process, the known parameters include P_{s_ref}, P_s, Q_{s_ref}, Q_s, u_{dc_ref}, u_{dc}, i_{dr}, i_{qr}, i_{ds}, i_{qs}, u_{ds}, u_{qs}, u_{dr}, u_{qr}, u_{dg}, and u_{qg}. The parameters to be identified include electrical parameters (L_s, L_r, L_m, and L_g), rotor winding resistance (R_r), stator winding resistance (R_s), and parameters of the converter PI controller.

It is shown that PI controller parameters are important for sensitivity analysis [24,25]. Therefore, the parameters to be identified for the DFIG converter control system are k_{p1},

$k_{p2} \ldots k_{p7}$ and $k_{i1}, k_{i2} \ldots k_{i7}$ in Equations (3) and (4). In the DFIG control system, parameters are generally set as follows: $k_{p2} = k_{p4}$, $k_{i2} = k_{i4}$, $k_{p6} = k_{p7}$, $k_{i6} = k_{i7}$ and $k_{i6} = k_{i7}$, so this setting is also used in this paper. The parameters to be identified for the back-to-back converter control system are shown in Tables 1 and 2.

Table 1. Parameters to be identified for the rotor-side converter (RSC).

Parameters to be Identified	Parameter Description
k_{p1}	Proportional parameters of the active power outer loop PI controller
ki_1	Integral parameters of the active power outer loop PI controller
k_{p2}	Proportional parameters of the rotor q-axis current inner loop PI controller
ki_2	Integral parameters of the rotor q-axis current inner loop PI controller
k_{p3}	Proportional parameters of the reactive power outer loop PI controller
ki_3	Integral parameters of the reactive power outer loop PI controller
k_{p4}	Proportional parameters of the rotor d-axis current inner loop PI controller
ki_4	Integral parameters of the rotor d-axis current inner loop PI controller

Table 2. Parameters to be identified for grid side converter (GSC).

Parameters to be Identified	Parameter Description
k_{p5}	Proportional parameters of the DC bus voltage outer loop PI controller
ki_5	Integral parameters of the DC bus voltage outer loop PI controller
k_{p6}	Proportional parameters of the grid-side current d-axis PI controller
ki_6	Integral parameters of the grid-side current d-axis PI controller
k_{p7}	Proportional parameters of the grid-side current q-axis PI controller
ki_7	Integral parameters of the rotor q-axis current inner loop PI controller

There are various operating modes of the DFIG, such as maximum power point tracking (MPPT) mode, constant speed mode, and constant power mode. In these modes, the control structure of the RSC and GSC are familiar, but the parameters may be different, which should be considered in the parameter identification method. Especially in the constant power mode, the blade angle of the DFIG will change. Because the blade controller only operates under specific wind speed conditions, even if the blade controller model is introduced here, the complexity of parameter identification method will not increase. Therefore, this paper only discusses the identification method of relevant parameters for the converter control system. Moreover, for generator parameter identification, it is mentioned in literature [17] that the greater the degree of disturbance, the higher are the accuracy of the identification results. Therefore, a certain disturbance should be applied to the DFIG at the beginning of parameter identification, and the data obtained in this way will make the identification results more accurate.

2.2. Identification of Converter Control Parameters in the Absence of Certain Variables

Data for certain variables corresponding to some key working conditions for parameter identification may be missing or contain errors occasionally. The parameter identification method in this case has to be considered. In a group of variables, there is usually a situation where one type of variable is not available, such as rotor current, stator current, stator voltage, or rotor-side or grid-side voltage.

In actual working conditions, because the excitation voltage on the rotor side of the doubly fed fan is not collected, the rotor side voltage is missing. Figure 2 shows that the loss of rotor-side voltage will only affect the solution of the RSC equations. During the parameter identification of DFIG, in the description equation of the RSC, the flux linkage equation, the voltage equation, and the state equation are substituted into the

output equation so as to eliminate the variable of the rotor-side voltage. Expressions of the rotor-side simultaneous equations are shown in Equation (5).

$$\begin{cases} \frac{dx_1}{dt} = P_{s\_ref} - P_s \\ \frac{dx_2}{dt} = \frac{dx_1}{dt}(k_{p1} + \frac{k_{i1}}{s})(-\frac{L_s}{L_m}) - i_{qr} \\ \frac{dx_3}{dt} = Q_{s\_ref} - Q_s \\ \frac{dx_4}{dt} = \frac{dx_3}{\mathrm{dt}}(k_{p3} + \frac{k_{i3}}{s})(-\frac{L_s}{L_m}) + \frac{U_s}{\omega_1 L_m} - i_{dr} \\ \frac{dx_4}{dt}(k_{p4} + \frac{k_{i4}}{s}) = \frac{d\psi_{dr}}{dt} + R_r i_{dr} \\ \frac{dx_2}{dt}(k_{p2} + \frac{k_{i2}}{s}) = \frac{d\psi_{qr}}{dt} + R_r i_{qr} \\ \psi_{dr} = L_r i_{dr} + L_m i_{ds} \\ \psi_{qr} = L_r i_{qr} + L_m i_{qs} \end{cases} . \quad (5)$$

According to Equation (5), the parameters to be identified are electrical parameters (L_m, L_r, L_s, R_r) and controller parameters (k_{p1}, k_{i1}, k_{p2}, k_{i2}, k_{p3}, k_{i3}, k_{p4}, k_{i4}). Other types of variables missing can also be handled in a similar way.

3. Hybrid Genetic Algorithm for Converter Control System Identification

At present, the swarm intelligence algorithms mainly used in wind power parameter identification research problems include the genetic algorithm, particle swarm algorithm, ant colony algorithm, differential evolution algorithm. The use of these algorithms alone in parameter identification will inevitably lead to some shortcomings and limitations. For example, the genetic algorithm easily falls into the local optimum when solving the objective function in parameter identification. The particle swarm algorithm highlights strong robustness in the process of use; however, the initial parameter setting relies on experience and experimentation. The differential evolution algorithm highlights the characteristics of strong robustness during use and exhibits a high degree of parallelism, but it easily falls into premature convergence. Moreover, the early convergence of the ant colony algorithm is relatively low. It is fast and has high precision, but it lacks effective mutation measures, the convergence is slow in the later stage, and the algorithm easily falls into the local optimum. In addition, the parameter identification model becomes complicated in the absence of key information such as rotor current, rotor voltage, stator current, stator voltage, grid-side current, and grid-side voltage, which makes the identification process easier for a single group of intelligent algorithms stuck in a local optimum. Based on this, an identification method for the control parameters of the DFIG converter based on the hybrid genetic algorithm is proposed in this paper.

3.1. Hybrid Genetic Algorithm

Genetic algorithm (GA) is a global optimization search algorithm based on evolutionary mechanisms such as good and bad selection and genetic variation in the process of biological survival [26]. GA mainly realizes the problem-solving process through four basic operations: reproduction, mutation, competition, and selection. Compared with the least-squares method, GA does not need to consider the influence of the initial value of the function for the identification results, and only needs to get the form of all objective functions to obtain the optimal solution [27].

The immune algorithm (IM) is proposed based on the diversity of the immune system and the learning and memory mechanism, which can be simulated by the recognition and binding between antibodies and antigens in the immune system and the production of antibodies [28].

The hybrid genetic algorithm proposed in this paper introduces an immune strategy and generation gap value, and retains the elite individuals in the population in the memory bank. The elite individuals are no longer genetically manipulated to ensure that each

chromosome has immune memory function. Then, the excellent genes in the individual are retained in the iterative process so as to improve the convergence speed and avoid falling into local solutions. The specific steps of the hybrid genetic algorithm include population initialization, calculating the population fitness value, calculating affinity, calculating the concentration of antibodies, and calculating the expected reproduction rate of antibodies.

3.1.1. Calculating Affinity

Affinity represents the binding degree between the antigen and antibody, which correspond to the objective function and feasible solution of the objective function, respectively [25]. Obtaining the affinity between the antibody and antigen in the genetic algorithm is done to calculate the individual fitness value (F_v). The greater the value of F_v, the greater the affinity. The affinity between the antibody and antibody in the hybrid genetic algorithm is the approximation between two chromosomes.

Whether the absolute error between the fitness values of the two individuals is less than a certain threshold (ε) is used to judge the similarity between two antibodies. As shown in Equation (6), if it is less than ε, the two individuals are considered to be approximately the "same", so $S_{v,s} = 1$; otherwise, the two individuals are different, so $S_{v,s} = 0$.

$$S_{i,j} = \begin{cases} 1\ , & |F_{vi} - F_{vj}| \le \varepsilon \\ 0\ , & |F_{vi} - F_{vj}| > \varepsilon \end{cases}. \tag{6}$$

Here, F_{vi} and F_{vj} represent the fitness values of two individuals.

3.1.2. Calculation of the Concentration of Antibody

The antibody concentration C_v represents the ratio of individuals and their similar individuals in the current population to the total number of individuals [17], as shown in Equation (7).

$$C_v = \frac{\sum\limits_{j \in N} S_{v,s}}{N}. \tag{7}$$

Here, N is the total number of antibodies, and j is the number of similar individuals of an individual. $S_{v,s}$ represents the degree of similarity between individual v and s. If the value of Equation (7) is 1, it means that the two individuals are similar; otherwise, if it is 0, they are different.

3.1.3. Calculation of the Expected Reproduction Rate of the Antibody

The expected reproduction rate of antibodies is used to promote the inheritance and variation of superior antibodies and ensure the diversity of antibodies. The expected reproduction probability of the antibody is determined by the fitness value (F_v) and the concentration (C_v) of the antibody; that is,

$$\begin{cases} P = \alpha \frac{\Delta y}{\sum \Delta y} + (1 - \alpha) \frac{C_v}{\sum C_v} \\ \Delta y = \frac{1}{F_v} \end{cases}, \tag{8}$$

where α is a constant value, and the deviation value (Δy) is the inverse value of the fitness value (F_v). According to Equation (8), the individual fitness value, deviation value, and individual concentration will affect the expected reproduction probability.

3.2. Application of Hybrid Genetic Algorithm for DFIG Control System Identification

The parameter identification of the DFIG control system needs to fit the actual output curve and model output curve. The smaller the difference between the two sets of curves, the closer the identified parameters are to the actual values. Therefore, in the parameter

identification of the DFIG converter control system, the fitness calculation function used is as follows:

$$\begin{cases} F_v = \frac{1}{\Delta y} \\ \Delta y = \sqrt{\frac{\sum_{i=1}^{n}\left[y_d(i) - y_{d_{data}}(i)\right]^2}{n}} + \sqrt{\frac{\sum_{i=1}^{n}\left[y_q(i) - y_{q_{data}}(i)\right]^2}{n}} \end{cases}, \quad (9)$$

where y_d and y_q are respectively the d-axis and q-axis response curves of the actual controller output; $y_{d_{data}}$ and $y_{q_{data}}$ are respectively the d-axis and q-axis output simulation curves of the identified model; and n represents the number of curve data.

As shown in Figure 2, both the RSCs and GSCs include current inner loop control blocks containing parameters $k_{p4} = k_{p2}$, $k_{i4} = k_{i2}$, $k_{p7} = k_{p6}$ and $k_{i7} = k_{i6}$. Therefore, the strategy of "individual identification, elite retention, and overall identification" will be adopted for parameter identification.

When identifying the parameters of the DFIG converter control system, the real number coding method is chosen to initialize the population. Taking the RSC as an example, the flow chart of the hybrid genetic algorithm in parameter identification of RSC of the DFIG is shown in Figure 3, and the corresponding steps are as follows:

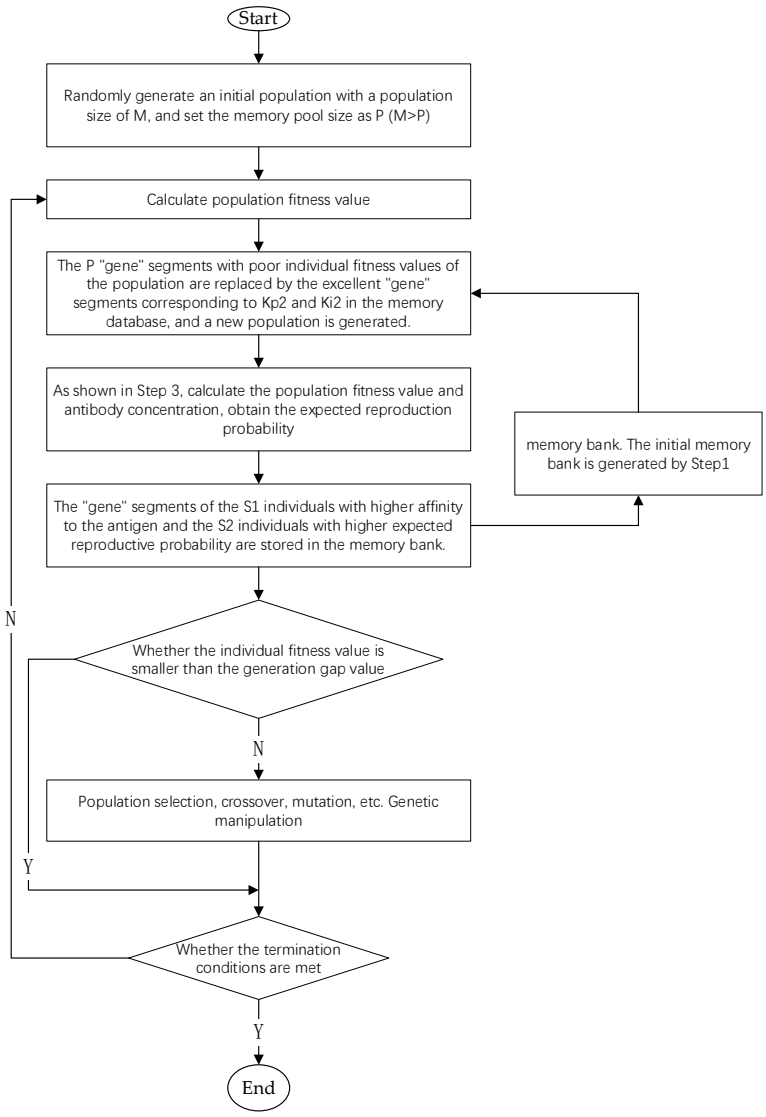

Figure 3. Flow chart for parameter identification of rotor-side converter.

Step 1: A separate fitting strategy for the d-axis and q-axis is adopted for the RSC. The evolutionary generations in the genetic algorithm are set as m_1 ($m_1 > 5$). The elite retention strategy is adopted, and the top five individuals with the highest fitness in the population are selected as elite individuals after one operation. The "gene" fragments corresponding to k_{p2} and k_{i2} in these five individuals are extracted and averaged to obtain a group of excellent "gene" fragments. Thus, n_1 groups of excellent "gene" fragments will be obtained from the d-axis and q-axis. These "gene" fragments will be used as the initial memory bank of the algorithm. The memory bank is set to be composed of $P = 2 * n_1$ individuals.

Step 2: The overall identification strategy of the d-axis and q-axis is adopted. The evolutionary algebra in the genetic algorithm [29] is set to M_1, and the initial population has M ($M > P$) randomly generated individuals. The fitness value of these M individuals is calculated by Equation (9). The "gene" fragments corresponding to k_{p2} and k_{i2} in the P individuals with the lowest fitness are replaced with excellent "gene" fragments in the memory bank.

Step 3: The expected reproductive probability of the antibody in the parent population is calculated. First, the concentration of the antibody is calculated by Equations (6) and (7). Then, the expected reproduction probability of the antibody is obtained with Equation (8).

Step 4: Progeny populations are produced. When updating the memory bank, the "gene" fragments corresponding to k_{p2} and k_{i2} in s_1 individuals with higher fitness values are first stored in the memory bank. According to the expected reproduction probability of the remaining individuals in the population, the "gene" segments corresponding to k_{p2} and k_{i2} in the $s_2 = P\text{-}s_1$ individuals with a high expected reproduction probability are stored in the memory bank.

Step 5: The fitness value and deviation value (Δ_y) of all individuals in the current population are calculated. Comparing Δ_y with the generation gap (σ), those with $\Delta y < \sigma$ are set as elite individuals and directly retained, while those with $\Delta y > \sigma$ go to the next genetic operation.

Step 6: The non-elite individuals in step 5 are put in order. Non-elite individuals evolve through selection, crossover, and mutation [29]. In the selection operation, the details are shown in Equation (8).

Step 7: If the termination conditions are met, the current individual value is output; otherwise, step 2 is followed.

Step 8: The above processes from step 2 to step 6 are run for n_1 times with the initial memory unchanged, and the running results to reduce the error are averaged.

The structure of the GSC is basically similar to that of the RSC, and so are the identification steps.

4. Test Case

The following test was used to evaluate the effectiveness of the proposed hybrid genetic algorithm. The operating conditions of MPPT, constant power, and constant speed were tested based on the simulation model (Section 4.1). The missing variables of rotor current, rotor voltage, stator current, stator current, stator voltage, and grid-side voltage were tested based on the simulation model (Section 4.2). Recorded data from a wind farm in Zhangjiakou, China, under the rotor voltage variable missing condition, were examined under power oscillation conditions (Section 4.3).

4.1. Simulation Test of Converter Parameter Identification under Three Operating Conditions

DFIG data with a wind speed of 8 m/s, 10.5 m/s, and 12.5 m/s, and fluctuation value of 1 m/s, 0.4 m/s, and 1 m/s were used for the test of MPPT, constant speed, and constant power operation conditions, respectively. The data of rotor current, rotor voltage, stator current, stator voltage, grid-side current, and grid-side voltage were used.

Taking the PI controller of the RSC as an example, the identification strategy of "individual identification, elite retention, and overall identification" was adopted. The basic parameters of the hybrid genetic algorithm were set as follows: evolutionary algebra

m_1 = 20, number of runs n_1 = 5, number of memory bank individuals P = 10, M = 30, threshold ε = 1; s_1 = 7, s_2 = 3, and generation gap σ = 0.05.

The basic parameter settings for parameter identification of GSCs were basically the same as those of RSCs. In the running state of MPPT, the comparison of the identification results between genetic algorithm and hybrid genetic algorithm is shown in Figure 4. The identification results of the converter in the constant speed region and the constant power region also converged when the evolutionary algebra was 20. As shown in Figure 4, in the subsequent iterations, because the fitness of the new offspring was not as good as the fitness value of the parent, the algorithm would retain the parent population and discard the offspring population, so the final identification curve was a straight line, representing the optimal value searched by the algorithm at this time. Because the genetic algorithm had problems such as local optimality, after a certain number of iterations, the genetic algorithm could not jump out of the local optimality and could not find the global optimal solution, which produced a large error in the parameter identification result.

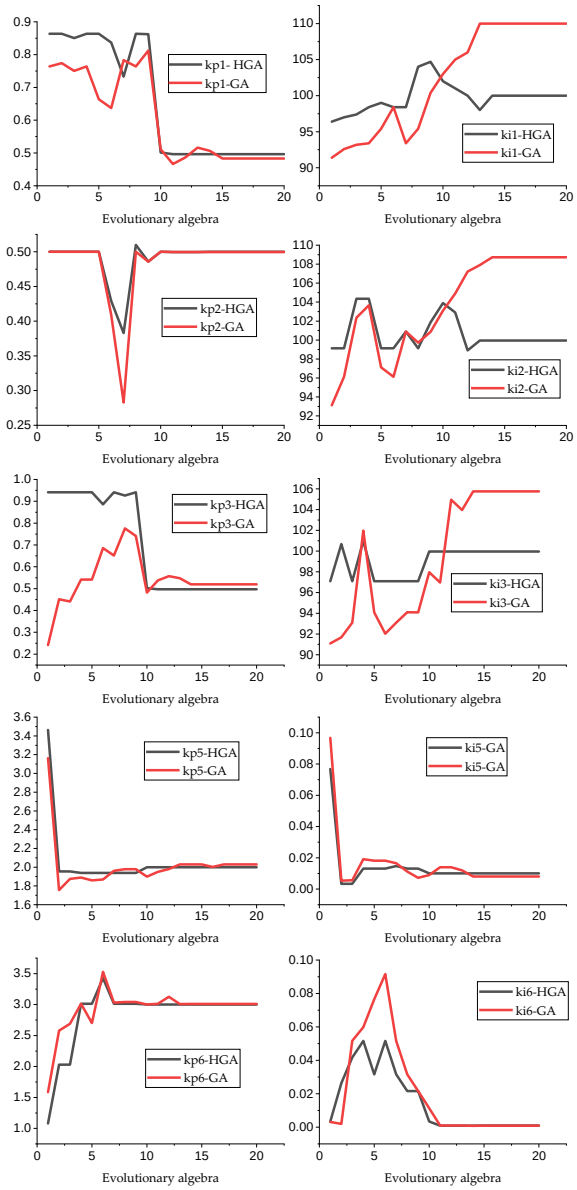

Figure 4. Comparison of identification results of the converter at the lower side of Maximum Power Point Tracking (MPPT).

Parameter identification results of the DFIG, RSC, and GSC under different operation conditions are shown in Tables 3 and 4, respectively.

Table 3. Identification results of RSC parameters in different control modes.

Operating Area	Algorithm	k_{p1}	k_{i1}	k_{p2}	k_{i2}	k_{p3}	k_{i3}
MPPT	actual value	0.5	100	0.5	100	0.5	100
	GA	0.4831	110.1348	0.4916	108.7231	0.5195	105.7642
	HGA	0.5001	99.9948	0.5000	99.9555	0.4995	100.0036
constant speed	GA	0.5063	103.0831	0.5011	99.5462	0.4969	100.1028
	HGA	0.5003	100.0700	0.5000	99.9641	0.4997	100.0049
constant power	GA	0.4824	102.7250	0.5113	108.2004	0.4893	98.0537
	HGA	0.4997	100.0030	0.5000	100.0073	0.5006	99.9974

Table 4. Identification results of GSC parameters in different control modes.

Operating Area	Algorithm	k_{p5}	k_{i5}	k_{p6}	k_{i6}
MPPT	actual value	2	0.01	3	0.001
	GA	2.004	0.0080	3.010	0.00087651
	HGA	2.000	0.01	3.000	0.00099918
constant speed	GA	2.001	0.0105	3.004	0.0009228
	HGA	2.000	0.01	3.000	0.0009458
constant power	GA	2.010	0.0103	3.006	0.0009022
	HGA	2.000	0.01	3.000	0.0009913

Among them, the parameters $k_{p4} = k_{p2}$, $k_{i4} = k_{i2}$; $k_{p7} = k_{p6}$, $k_{i7} = k_{i6}$.

It can be seen from Tables 3 and 4 that the hybrid genetic algorithm could identify the key parameters of the DFIG converter control systems effectively, as well as whether DFIG was in MPPT operation condition, constant speed operation condition or constant power operation condition. In addition, for the same set of control system parameters, the identification results are not consistent under different operation conditions. As the identification result of MPPT operation condition is closest to the actual value, the operation data in MPPT condition can be preferentially selected for practical engineering application.

4.2. Simulation Test of Converter Parameter Identification in the Absence of Variables

From the analysis in Section 4.1, it is known that the parameter identification results obtained by applying the data of DFIG in MPPT operation conditions are more accurate. Therefore, MPPT is used as a typical operating condition to test the effect of converter parameter identification under the variable missing condition. Based on the simulation model, the data of rotor current, rotor voltage, stator current, stator voltage, grid-side current, and grid-side voltage corresponding to the wind turbine in the MPPT operation condition were generated. Then, by simulating the missing data of rotor current, rotor voltage, stator current, stator voltage, grid-side current, or grid-side voltage data, the hybrid genetic algorithm proposed in this paper was used to identify the parameters of the DFIG converter.

4.2.1. Missing Rotor Current

When the rotor currents i_{dr} and i_{qr} were missing, according to Figure 2, the absence of rotor current did not affect the parameter identification of the GSC, but did affect the parameter identification process of the machine-side converter. Taking the unknown electrical parameters L_s and L_r and the L_m converter parameters k_{p1} k_{i1}, k_{p2}/k_{p4}, k_{i2}/k_{i4}, k_{p3}, and k_{i3} as unknown important parameters, the hybrid genetic algorithm was used to identify these unknown parameters. The identification results of electrical parameters and controller parameters are shown in Tables 5 and 6, respectively.

Table 5. Identification results of electrical parameters.

Electrical Parameter	L_s	L_r	L_m
actual value (pu)	0.0049	0.0049	0.0045
identification value (pu)	0.0051	0.0047	0.0044

Table 6. Identification of rotor-side control parameters.

Control Parameter	k_{p1}	k_{i1}	k_{p2}	k_{i2}	k_{p3}	k_{i3}
actual value	0.5	100	0.5	100	0.5	100
identification value	0.4962	102.5231	0.4899	99.8759	0.5043	103.4254

Among them, the default $k_{p2} = k_{p4}$, $k_{i2} = k_{i4}$.

4.2.2. Missing Stator Current

When the stator current i_{ds} and i_{qs} were missing, the situation was basically the same as the rotor current missing. When the stator current was missing, it is shown in Figure 2 that it did not affect the identification process of GSC parameters, only the process of machine-side converter parameter identification. The electrical unknown parameters were L_s, $L_{r,}$ and L_m, and the remaining unknown parameters were the controller parameters k_{p1}, k_{i1}, k_{p2}/k_{p4}, k_{i2}/k_{i4}, k_{p3}, and k_{i3}. Therefore, a strategy of identifying the two sets of parameters as unknown parameters was adopted. The specific identification results are shown in Tables 7 and 8.

Table 7. Identification results of electrical parameters.

Electrical Parameters	L_s	L_r	L_m
actual value (pu)	0.0049	0.0049	0.0045
identification value (pu)	0.0043	0.0043	0.0048

Table 8. Identification of rotor-side control parameters.

Control Parameter	k_{p1}	k_{i1}	k_{p2}	k_{i2}	k_{p3}	k_{i3}
actual value	0.5	100	0.5	100	0.5	100
identification value	0.4912	99.6518	0.5145	99.1584	0.4899	99.5214

Among them, the default $k_{p2} = k_{p4}$, $k_{i2} = k_{i4}$.

4.2.3. Missing Grid-Side Converter Voltage

When the grid-side converter voltages u_{dg} and u_{qg} were missing, it can be seen from Figure 2 that the situation at this time was different from the situation in which the stator and rotor currents were missing. The GSC voltage loss would only affect the GSC. The identification of the parameters would not affect the identification of the parameters of the machine-side converter. When fitting the unknown parameters, only the grid-side filter inductance L_g was unknown for the electrical parameters, and the other unknown parameters were the controller parameters k_{p5}, k_{i5}, k_{p6}/k_{p7}, k_{i6}/k_{i7}, so the grid-side filter inductance L_g was the same as the grid-side controller. The parameters were identified together as unknown parameters. The results of parameter identification are shown in Tables 9 and 10.

Table 9. Identification results of electrical parameters.

Electrical Parameters	L_g
actual value (pu)	0.0040
identification value (pu)	0.0038

Table 10. Identification of grid-side control parameters.

Control Parameter	k_{p5}	k_{i5}	k_{p6}	k_{i6}
actual value	2	0.01	3	0.001
identification value	1.999	0.0098	3.001	0.00099

Among them, the default $k_{p7} = k_{p6}$, $k_{i7} = k_{i6}$.

4.2.4. Missing Stator Voltage

When the stator voltages u_{ds} and u_{qs} were missing, according to the structure of the machine-side converter and the structure of the grid-side converter in Figure 2, the absence of the stator voltage would affect the parameter identification of the machine-side converter and the GSC. Therefore, it was necessary to replace the stator voltage u_{ds} and u_{qs} in the output items of the machine-side converter and the GSC so as to complete the parameter identification research of the converter control system of the DFIG based on the absence of the stator voltage. As the structure of the GSC is simpler than that of the machine-side converter, when the parameters of the grid-side converter were first identified, at this time, the unknown parameters were the electrical parameters (L_m, L_r, L_s, and L_g) and controller parameters (k_{p5}, k_{i5}, k_{p6}/k_{p7}, k_{i6}/k_{i7}). The identification results are shown in Tables 11 and 12.

Table 11. Identification results of electrical parameters.

Electrical Parameters	L_s	L_g	L_m	L_r
actual value (pu)	0.0049	0.0040	0.0045	0.0049
identification value (pu)	0.0043	0.0048	0.0044	0.0049

Table 12. Identification of grid-side control parameters.

Control Parameter	k_{p5}	k_{i5}	k_{p6}	k_{i6}
actual value	2	0.01	3	0.001
identification value	1.898	0.0091	3.105	0.0015

Then, the machine-side converter was identified, and the parameters to be identified were the controller parameters k_{p1}, k_{i1}, k_{p2}/k_{p4}, k_{i2}/k_{i4}, k_{p3}, and k_{i3}. The identification results are shown in Table 13.

Table 13. Identification of rotor-side control parameters.

Control Parameter	k_{p1}	k_{i1}	k_{p2}	k_{i2}	k_{p3}	k_{i3}
actual value	0.5	100	0.5	100	0.5	100
identification value	0.4756	97.3581	0.5205	105.1554	0.5199	104.9518

Among them, the default $k_{p2} = k_{p4}$, $k_{i2} = k_{i4}$.

4.2.5. Missing Rotor-Side Voltage

When the rotor-side voltages u_{dr} and u_{qr} were missing, according to Figure 2, the absence of rotor-side voltages u_{dr} and u_{qr} did not affect the parameter identification of the GSC, but only affected the parameters of the machine-side converter. At this time, new unknown parameters would appear as stator resistance (Rs) and stator winding inductance (L_s). The electrical parameters L_m, R_s, L_s, identification results, and process are shown in Table 14.

Table 14. Identification results of electrical parameters.

Electrical Parameters	L_m	L_s	R_s
actual value (pu)	0.0045	0.0049	0.002
identification value (pu)	0.0046	0.0050	0.00199

Then, the strategy of identifying R_r and L_r together with the controller parameters k_{p1}, k_{i1}, k_{p2}/k_{p4}, k_{i2}/k_{i4}, k_{p3} and k_{i3} was adopted. The identification results are shown in Table 15.

Table 15. Identification results of electrical parameters.

Electrical Parameters	R_r	L_r
actual value (pu)	0.001	0.0049
identification value (pu)	0.0012	0.0049

Then, the machine-side converter was identified, and the parameters to be identified were the controller parameters k_{p1}, k_{i1}, k_{p2}/k_{p4}, k_{i2}/k_{i4}, k_{p3}, and k_{i3}. The identification results are shown in Table 16.

Table 16. Identification of rotor-side control parameters.

Control Parameter	k_{p1}	k_{i1}	k_{p2}	k_{i2}	k_{p3}	k_{i3}
actual value	0.5	100	0.5	100	0.5	100
identification value	0.5011	99.9878	0.5002	99.6645	0.4992	100.0125

Among them, the default $k_{p2} = k_{p4}$, $k_{i2} = k_{i4}$.

4.3. Engineering Application

A DFIG wind farm in Zhangjiakou of North China was selected as the test case. Figure 5 shows recorded data of the DFIG under the condition of power oscillation, where the time length was 21 s, and the sampling period was 0.01 s, wherein the rotor-side voltages u_{dr} and u_{qr} were missing.

In the absence of the rotor-side voltages u_{dr} and u_{qr}, the identification results are shown in Tables 17–19, in which the assumption of $k_{p4} = k_{p2}$, $k_{i4} = k_{i2}$, $k_{p7} = k_{p6}$ and $k_{i7} = k_{i6}$ was still adopted.

Table 17. Identification of DFIG generator parameters.

Unknown Parameter	R_s	L_s	L_m	R_r	L_r
identification value (pu)	0.022	4.857	4.68	0.026	4.796

Table 18. Identification of rotor-side control parameters.

Unknown Parameter	k_{p1}	k_{i1}	k_{p2}	k_{i2}	k_{p3}	k_{i3}
identification value (pu)	0.001	5.425	0.0242	2.001	0.001	4.996

Table 19. Identification of grid-side control parameters.

Unknown Parameter	k_{p5}	k_{i5}	k_{p6}	k_{i6}
identification value (pu)	2.158	20.751	5.056	2.000

Applying the identified parameters, a set of curves was obtained from the DFIG simulation model, and the comparison made with the original recorded data is shown in

Figure 5. It can be seen from Figure 6 that the amplitude and phase of the original data and the simulated power curve were extremely close, indicating that the identification results are relatively close to the actual values.

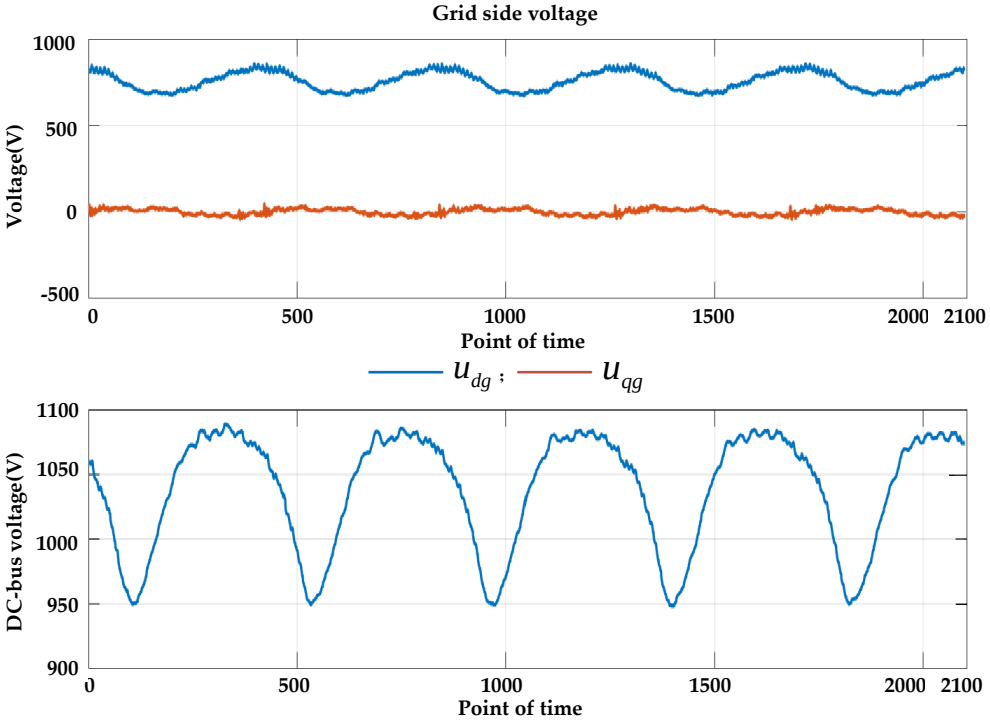

(**a**) voltage variables of U_{dg}, U_{qg}, and DC-bus voltage U_{dc}

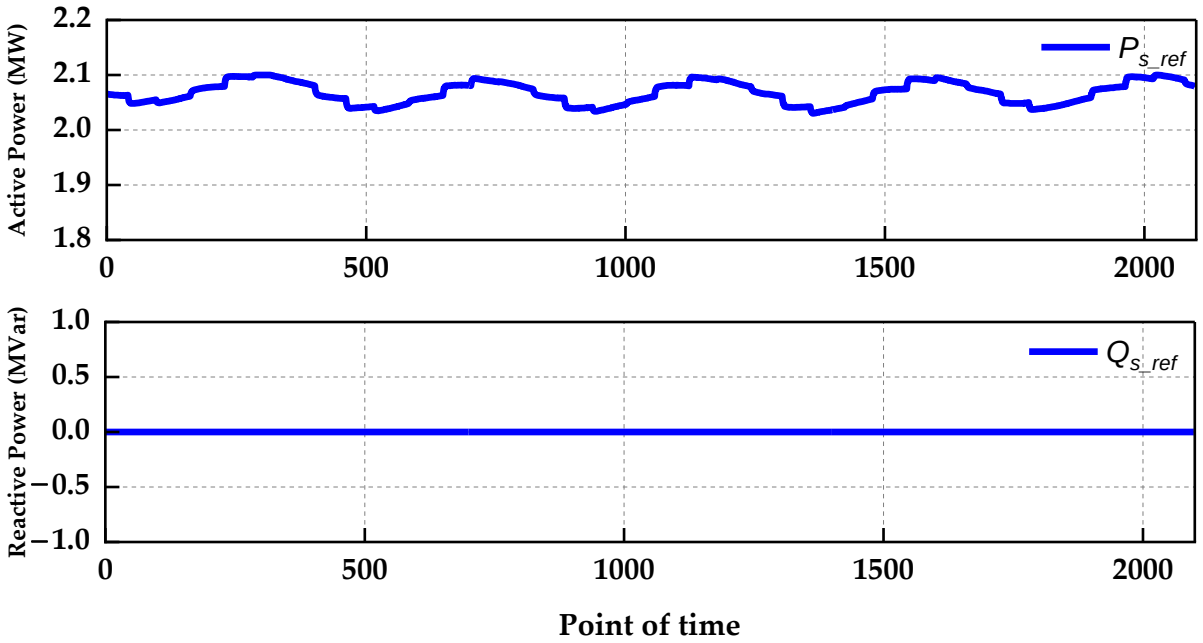

(**b**) reference variables of P and Q

Figure 5. *Cont.*

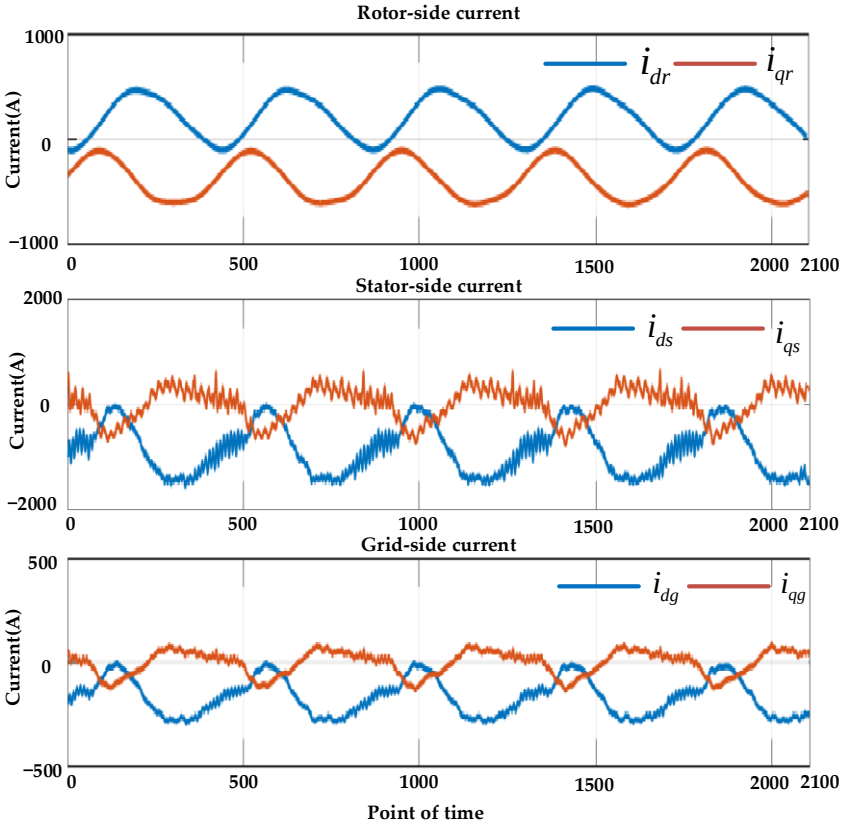

(**c**) current variables of I_{dg}, I_{qg}, I_{ds}, I_{qs}, $I_{dr,}$ and I_{qr}

Figure 5. DFIG variables under the condition of power oscillation.

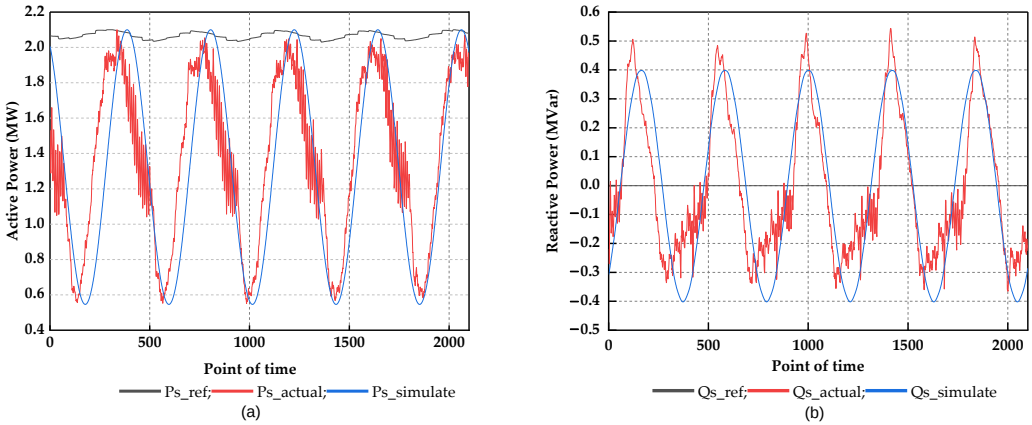

Figure 6. Comparison chart of the actual power curve and simulated power curve. (**a**) Comparison chart of the actual active power curve and simulated active power curve; (**b**) Comparison chart of the actual reactive power curve and simulated reactive power curve.

5. Conclusions

A hybrid genetic algorithm for parameter identification of the DFIG control system was proposed. The algorithm introduces the generation gap value and immune strategy, and adopts the identification strategy of "individual identification, elite retention, and overall identification." The test case showed that the identification results are different under different DFIG operating conditions, and the identification results under the MPPT operating condition are preferable.

According to the engineering requirements of parameter identification, we discussed the lack of DFIG variables, such as rotor voltage, rotor current, stator voltage, stator current,

and grid-side voltage. If one of the variables is missing, the DFIG converter control system parameters can still be identified by the proposed method.

Author Contributions: Conceptualization, methodology, validation, writing—review and editing, L.W.; methodology, data curation, validation, writing—review and editing, H.L.; investigation, validation, supervision, writing—review and editing, J.Z.; software, visualization, writing—review and editing, C.L.; data curation, investigation, writing—review and editing, Y.S.; supervision, writing—review and editing, Z.L.; investigation, software, validation, J.L. All authors have read and agreed to the published version of the manuscript.

Funding: This work was supported by the science and technology project "Electromagnetic Transient Simulation Initialization Program and Simulation Data Visualization Software Development" of North China Electric Power Research Institute Co., Ltd, Beijing, China [grant number SGTYHT/21-JS-225].

Institutional Review Board Statement: Not applicable.

Informed Consent Statement: Not applicable.

Data Availability Statement: Not applicable.

Conflicts of Interest: The authors declare no conflict of interest.

References

1. Jia, K.; Gu, C.; Li, L.; Xuan, Z.; Bi, T.; Thomas, D. Sparse voltage amplitude measurement based fault location in large-scale photovoltaic power plants. *Appl. Energy* **2018**, *211*, 568–581. [CrossRef]
2. Kim, D.; El-Sharkawi, M.A. Dynamic equivalent model of wind power plant using parameter identification. *IEEE Trans. Energy Convers.* **2016**, *31*, 37–45. [CrossRef]
3. Jin, Y.; Lu, C.; Ju, P.; Rehtanz, C.; Wu, F.; Pan, X. Probabilistic Preassessment Method of Parameter Identification Accuracy with an Application to Identify the Drive Train Parameters of DFIG. *IEEE Trans. Power Syst.* **2020**, *35*, 1769–1782. [CrossRef]
4. Abdelrahem, M.; Hackl, C.; Kennel, R. Application of extended Kalman filter to parameter estimation of doubly-fed induction generators in variable-speed wind turbine systems. In Proceedings of the International Conference on Clean Electrical Power (ICCEP), Taormina, Italy, 16–18 June 2015.
5. Belmokhtar, K.; Ibrahim, H.; Merabet, A. Online parameter identification for a DFIG driven wind turbine generator based on recursive least squares algorithm. In Proceedings of the IEEE 28th Canadian Conference on Electrical and Computer Engineering, Halifax, NS, Canada, 3–6 May 2015.
6. Kong, M.; Sun, D.; He, J.; Nian, H. Control Parameter Identification in Grid-side Converter of Directly Driven Wind Turbine Systems. In Proceedings of the 12th IEEE PES Asia-Pacific Power and Energy Engineering Conference (APPEEC), Nanjing, China, 20–23 September 2020.
7. Wang, X.; Xiong, J.; Geng, L.; Zheng, J.; Zhu, S. Parameter identification of doubly-fed induction generator by the Levenberg-Marquardt-Fletcher method. In Proceedings of the IEEE Power & Energy Society General Meeting, Vancouver, BC, Canada, 21–25 July 2013.
8. Takahashi, K.; Matayoshi, H.; Senjyu, T.; Takahashi, H.; Howlader, A.M. Online Parameter identification of PMSG Wind turbine for Output Power control. In Proceedings of the TENCON 2019–2019 IEEE Region 10 Conference (TENCON), Kochi, India, 17–20 October 2019.
9. Zhang, C.; Allafi, W.; Dinh, Q.; Ascencio, P.; Marco, J. Online estimation of battery equivalent circuit model parameters and state of charge using decoupled least squares technique. *Energy* **2018**, *142*, 678–688. [CrossRef]
10. Xia, B.; Lao, Z.; Zhang, R.; Tian, Y.; Chen, G.; Sun, Z.; Wang, W.; Sun, W.; Lai, Y.; Wang, M.; et al. Online parameter identification and state of charge estimation of Lithium-Ion batteries based on forgetting factor recursive least squares and nonlinear kalman filter. *Energies* **2018**, *11*, 3. [CrossRef]
11. Zhao, Q.; Wu, L.; Wang, X.; Sheng, S.; Feng, Z. Overview of research on modelling and parameter identification of wind power generator. In Proceedings of the 16th IET International Conference on AC and DC Power Transmission (ACDC 2020), Online Conference, 2–3 July 2020.
12. Rong, Y.; Wang, H.; Yang, W.; Qi, H. Artificial neural network in the application of the doubly-fed type wind power generator parameter identification. In Proceedings of the IEEE Conference and Expo Transportation Electrification Asia-Pacific (ITEC Asia-Pacific), Beijing, China, 31 August–3 September 2014.
13. Chen, H.; Liu, H.; Chu, X.; Liu, Q.; Xue, D. Anomaly detection and critical SCADA parameters identification for wind turbines based on LSTM-AE neural network. *Renew. Energy* **2021**, *172*, 829–840. [CrossRef]
14. Li, Y.; Yang, J.; Yi, B.; Fang, R.; Zhang, D. Dynamic equivalence of doubly-fed wind turbines based on parameter identification and optimization. In Proceedings of the 4th International Conference on Mechatronics and Computer Technology Engineering (MCTE 2021), Xi'an, China, 15–17 October 2021.

15. Pan, X.; Ju, P.; Wu, F.; Jin, Y. Hierarchical parameter estimation of DFIG and drive train system in a wind turbine generator. *Front. Mech. Eng.* **2017**, *12*, 367–376.
16. La Cava, W.; Danai, K.; Spector, L.; Fleming, P.; Wright, A.; Lackner, M. Automatic identification of wind turbine models using evolutionary multiobjective optimization. *Renew. Energy* **2016**, *87*, 892–902. [CrossRef]
17. Liu, J.Z.; Guo, J.L.; Hu, Y.; Wang, J.; Liu, H. Dynamic modeling of wind turbine generation system based on grey-box identification with genetic algorithm. In Proceedings of the 36th Chinese Control Conference (CCC), Dalian, China, 26–28 July 2017.
18. Junxian, H.; Xiangyu, T.; Shi, Z.; Hong, S.; Haiyan, T.; Tao, L.; Peng, Z. The dynamic simulation model and parameter identification method of DFIG type wind generator for power system elec-tro-mechanic simulation. In Proceedings of the IEEE PES Asia-Pacific Power and Energy Engineering Conference (APPEEC), Hong Kong, China, 7–10 December 2014.
19. Gu, R.; Dai, J.; Zhang, J.; Miao, F.L.; Tang, Y. Research on Equivalent Modeling of PMSG-based Wind Farms using Parameter Identification method. In Proceedings of the 12th IEEE PES Asia-Pacific Power and Energy Engineering Conference (APPEEC), Nanjing, China, 2–3 July 2020.
20. Zhang, J.A.; Liu, H.F.; Liu, H.; Wu, L.; Wang, Y.H. Estimation of wind turbine parameters with piecewise trends identification. In Proceedings of the International Conference on Mechatronic Science, Electric Engineering and Computer (MEC), Shenyang, China, 20–22 December 2013.
21. Liu, X.; Yan, L.; Liu, Y.; Zhao, L.; Jie, J. Improved niche genetic algorithm based parameter identification of excitation system considering parameter identifiability. In Proceedings of the 14th IET International Conference on AC and DC PowerTransmission (ACDC 2018), Chengdu, China, 28–29 June 2018.
22. Li, S.; Haskew, T.A.; Jackson, J. Integrated power characteristic study of DFIG and its frequency converter in wind power generation. *Renew. Energy* **2010**, *35*, 42–51. [CrossRef]
23. Taveiros, F.E.V.; Barros, L.S.; Costa, F.B. Back-to-back converter state-feedback control of DFIG (doubly-fed induction generator)-based wind turbines. *Energy* **2015**, *89*, 896–906. [CrossRef]
24. Shen, W.; Li, H. A Sensitivity-Based Group-Wise parameter identification algorithm for the electric model of Li-Ion battery. *IEEE Access* **2017**, *5*, 4377–4387. [CrossRef]
25. Moshksar, E.; Ghanbari, T. Adaptive estimation approach for parameter identification of photovoltaic modules. *IEEE J. Photovolt.* **2017**, *7*, 614–623. [CrossRef]
26. Wasilewski, J.; Wiechowski, W.; Bak, C.L. Harmonic domain modeling of a distribution system using the DIgSILENT PowerFactory software. In Proceedings of the International Conference on Future Power Systems, Amsterdam, The Netherlands, 18 November 2005.
27. Li, W.; Chai, Z.; Tang, Z. A decomposition-based multi-objective immune algorithm for feature selection in learning to rank. *Knowl.-Based Syst.* **2021**, *234*, 107577.
28. Su, Y.; Luo, N.; Lin, Q.; Li, X. Many-objective optimization by using an immune algorithm. *Swarm Evol. Comput.* **2022**, *69*, 101026. [CrossRef]
29. Ganthia, B.P.; Barik, S.K.; Nayak, B. Genetic Algorithm Optimized and Type-I fuzzy logic controlled power smoothing of mathematical modeled Type-III DFIG based wind turbine system. *Mater. Today Proc.* 2021, *in press*.